

RESEARCH ARTICLE

Multi-scale vascularization strategy for 3D-bioprinted tissue using coaxial core-shell pre-set extrusion bioprinting and biochemical factors

Jae-Hun Kim¹, Minji Park², Jin-Hyung Shim^{2,3}, Won-Soo Yun^{2,3}, Songwan Jin^{2,3*}

¹Department of Mechanical System Engineering, Graduate School of Knowledge-based Technology and Energy, Tech University of Korea, Siheung-si, Gyeonggi-do, Republic of Korea

²T&R Biofab, Siheung-si, Gyeonggi-do, Republic of Korea

³Department of Mechanical Engineering, Tech University of Korea, Siheung-si, Gyeonggi-do, Republic of Korea

Abstract

Three-dimensional bioprinting is a key technology in bioartificial organ production. However, production of bioartificial organs has significant limitations because it is hard to build vascular structures, especially capillaries, in printed tissue owing to its low resolution. As the vascular structure plays a critical role in delivering oxygen and nutrients to cells and removing metabolic waste, building vascular channels in bioprinted tissue is essential for bioartificial organ production. In this study, we demonstrated an advanced strategy for fabricating multi-scale vascularized tissue using a pre-set extrusion bioprinting technique and endothelial sprouting. Using a coaxial precursor cartridge, mid-scale vasculature-embedded tissue was successfully fabricated. Furthermore, upon generating a biochemical gradient environment in the bioprinted tissue, capillaries were formed in this tissue. In conclusion, this strategy for multi-scale vascularization in bioprinted tissue is a promising technology for bioartificial organ production.

Keywords: 3D bioprinting; Biochemical gradient; Endothelial sprouting; Pre-set extrusion; Vascularized tissue

*Corresponding author:

Songwan Jin
(songwan@tukorea.ac.kr)

Citation: Kim J-H, Park M, Shim J-H, *et al.*, 2023, Multi-scale vascularization strategy for 3D-bioprinted tissue using coaxial core-shell pre-set extrusion bioprinting and biochemical factors. *Int J Bioprint*.
<https://doi.org/10.18063/ijb.726>

Received: December 21, 2022

Accepted: March 01, 2023

Published Online: April 4, 2023

Copyright: © 2023 Author(s).

This is an Open Access article distributed under the terms of the Creative Commons Attribution License, permitting distribution, and reproduction in any medium, provided the original work is properly cited.

Publisher's Note: Whioce Publishing remains neutral with regard to jurisdictional claims in published maps and institutional affiliations.

1. Introduction

The organ shortage crisis is a long-standing and deepening problem in organ transplantation^[1]. The most promising technology for addressing organ shortage is the production of bioartificial organs as a substitute for damaged or dysfunctional organs. However, methods to produce bioartificial organ such as genetically modified xenograft^[2], cell-laden biomaterial molding^[3], and recellularization of decellularized organ^[4] have problems such as latent immunoreaction, low reproducibility, and low resolution to precise positioning of multiple types of cells. Three-dimensional (3D) bioprinting is a promising technology in the field of bioartificial organ manufacturing, owing to the possibility of 3D patterning on a pre-designed position with a software-controlled

3D printing system. Emerging advancements in 3D bioprinting technology have shown high potential in the production of bioartificial tissues or organs^[5], such as the skin, cartilage, and heart.

Despite this, a considerable limitation of 3D bioprinting is the production of cell-laden large-volume tissue owing to the difficulty in formation of the hierarchical multi-scale vascular structure in tissue. The vascular structure is significantly important because the vascular tissue in the human body plays a critical role in carrying blood for delivering oxygen and nutrients to cells and removing metabolic waste products from them; additionally, capillaries improve the contact area of vascular tissue with surrounding tissue. Numerous studies have been conducted for building vasculatures in bioprinted tissues^[6]; however, they do not successfully mimic the hierarchical multi-scale vascular structure of native tissue, especially capillary branches, due to insufficient mechanical properties of the bioink, and low resolution result from physical limitations such as the printing nozzle size and the resolution of the bioprinter. Without vascular tissue in the bioprinted tissue, nutrients and oxygen can only be supplied to cells by diffusion. However, the diffusion coefficient is usually lowered in the printed construct, due to the presence of hydrogel fibers and cells, and most of the diffused oxygen and nutrients are taken up by cells at the surface of the construct. These combinations cause cell death in the center of the bioprinted tissue, which leads to the failure of its role as a bioartificial organ.

One of the most widely used methods for creating an artificial capillary branch is through a biochemical gradient demonstrated using a microfluidic device. In this method, endothelial cells were injected inside fabricated perfusion channels and then allowed to seed. After endothelialization of perfusion channels, endothelial sprouting is induced via the formation of a biochemical gradient associated with angiogenesis^[7]. This method enables the creation of perfusable capillaries that branch out from the endothelialized perfusion channel.

Here, we introduce a multi-scale vascularization strategy in bioprinted construct that combines 3D bioprinting technology and endothelial sprouting technique in microfluidic devices. To fabricate a mid-scale vasculature-embedded bioprinted tissue construct, we applied a pre-set extrusion bioprinting technique that has an advantage on fabrication of heterogeneous, multicellular, and precisely structured tissue with a simple extrusion-based bioprinting system^[8]. In a previous study, this technique was used for successfully fabricating a hepatic lobule-like structure with mid-scale vasculature^[9]. Using this strategy, mid-scale vasculature-embedded tissue

was printed in the insert of a transwell. Subsequently, a biochemical gradient comprising a cocktail of vascular endothelial growth factor (VEGF), phorbol 12-myristate 13-acetate, and sphingosine 1-phosphate, was generated in the bioprinted tissue to induce endothelial sprouting. As a result, we successfully fabricated a bioprinted tissue embedding multi-scale vascular architecture of mid-scale vasculatures and capillary branches capable of material transfer.

2. Materials and methods

2.1. Design and fabrication of precursor cartridges

First, for bioprinting tissue constructs embedding mid-scale vasculatures, precursor cartridges with coaxial architecture were designed using the 3D CAD software (Solidworks 2020, Dassault Systems, France). The 3D CAD file was converted into an STL file to import a 3D printing system. Precursor cartridges were fabricated using a photocrosslinkable resin (VisiJet SL Clear, 3D Systems, USA) and a 3D printer (Projet 6000, 3D Systems). The fabricated precursor cartridges were briefly rinsed with 70% ethanol and sterilized with ultraviolet light for 1 h before use.

2.2. Cell culture

The human dermal fibroblast cell line CCD-986Sk (CRL-1947, ATCC, USA) was cultured in Iscove's modified Dulbecco's medium (31980-030, Thermo Fisher Scientific, USA) supplemented with 10% fetal bovine serum. Primary human umbilical vein endothelial cells (HUVECs, C2517A, Lonza, Switzerland) were cultured in endothelial basal growth medium (CC-3156, Lonza) supplemented with EGM-2 SingleQuots (CC-4176, Lonza). All cells were cultured in an incubator (37°C, 5% CO₂), and the culture medium was changed every 2 days.

2.3. Preparation of bioink

For fabrication of cell-laden tissue, a commercial decellularized extracellular matrix (dECM) from porcine skin (deCelluid-skin, T&R Biofab, South Korea) was used in this study. The dECM bioink was prepared according to the manufacturer's instructions. Briefly, dECM sponge was dissolved in 0.5 M acetic acid solution for 72 h at 4°C in 3 wt%. Subsequently, acidic dECM solution was mixed with 10× minimum essential medium (11430-030, Thermo Fisher Scientific) at a volume ratio of 8:1. Subsequently, the mixed solution was neutralized with reconstitute buffer (1.1 g of NaHCO₃, 2.4 g of hydroxyethyl piperazine ethanesulfonic acid, and 7 g of NaOH in 50 mL of distilled water).

To build a mid-scale vasculature in the printed tissue, an alginate solution was used as a sacrificial hydrogel. Alginic acid sodium salt (A2033, Sigma-Aldrich, USA)

was dissolved in Dulbecco's phosphate-buffered saline (DPBS, LB001-02, WELGENE, South Korea) and stirred for 12 h at 25°C.

For printing cells, CCD-986Sk and HUVECs were detached from the culture dish using 0.25% trypsin-EDTA (25200-072, Thermo Fisher Scientific) and ReagentPack™ Subculture Reagents (CC-5034, Lonza). Next, CCD-986Sk (3×10^6 cells/mL) was mixed with dECM, and HUVECs (6×10^6 cells/mL) were mixed with 3.5% alginate solution. The bioinks were centrifuged at 2500 rpm at 4°C for 30 min for removing bubbles.

2.4. Assessment of pre-set extrusion bioprinting parameters

We presumed that the geometry of the precursor cartridge and concentration of the alginate solution critically influenced the diameter of the lumen in the bioprinted structure. To analyze the effect of these parameters on lumen diameter, we used cartridges with core region diameters of 1.4, 1.7, and 2.0 mm and 3.0, 3.5, and 4.0 wt% alginate solutions.

The dECM bioink and alginate bioink were loaded in a precursor cartridge, and the bioink-loaded precursor cartridge was placed into a 3-mL Luer lock syringe with an 18G nozzle. The bioinks were printed into prewarmed DPBS at 37°C using a pneumatic dispenser (S-Sigma-CM3-V2, Musashi Engineering, Japan) at a pressure of 7 kPa. Subsequently, gelation of the printed fibers was conducted in a CO₂ incubator for 30 min. After gelation, the fibers were sliced using a surgical blade. Images of the sliced fibers were obtained using an inverted microscope (CKX53, Olympus, Japan) with a CMOS camera (DP74, Olympus) and image acquisition software (CellSence, Olympus). The area of the lumen embedded in the printed fiber was measured using ImageJ v1.52 software, and the diameter of the lumen was calculated using Equation I:

$$\text{Diameter of lumen} = \sqrt{\frac{4 \times \text{Area of lumen}}{\pi}} \quad (\text{I})$$

2.5. Simulation of diffusion behavior through bioprinted tissue

To simulate the diffusion behavior of biochemicals in bioprinted tissues, we selected VEGF as a representative biochemical factor in this study. The diffusion coefficient of VEGF in the gelled dECM bioink was estimated by evaluating the diffusion of 40 kDa fluorescein isothiocyanate (FITC)-dextran (FD40S, Sigma-Aldrich), which has a molecular weight similar to that of VEGF (≈ 46 kDa). We prepared a gelled dECM block inside the PTFE tube and gently added FITC-dextran solution to establish direct contact with the gelled dECM. The opening of the PTFE tube was covered with paraffin. After 15 min, a

fluorescence image of the interface between the dECM bioink and FITC-dextran solution was obtained using a mercury lamp (U-HGLGPS, Olympus), sCMOS camera (Neo 5.5, Andor, UK), and inverted microscope (IX71, Olympus) using a 4× objective lens and FITC filter set. A one-dimensional intensity profile was obtained using the ImageJ software, and the fluorescence intensity of the FITC-dextran solution and the background was normalized to the maximum concentration of FITC-dextran solution and zero, respectively. The concentration profile obtained from experiment was fitted to the following one-dimensional diffusion mathematical equation (Equation II)^[10]:

$$c(x,t) = c_0 \cdot \operatorname{erfc} \left(\frac{x}{\sqrt{4 \cdot D_{\text{dECM}} \cdot t}} \right) \quad (\text{II})$$

In addition, the effective diffusion coefficient of VEGF (D_{medium}) in the culture medium was derived from the Stokes–Einstein equation (Equation III):

$$D_{\text{medium}} = \frac{k_b \cdot T}{6 \cdot \pi \cdot \eta \cdot r_h} \quad (\text{III})$$

We estimated that the viscosity of the culture medium (η) was not significantly different from that of water. In addition, r_h was calculated using Equation IV^[11]:

$$R_{\text{min}} = 0.066 \cdot M^{1/3} \quad (\text{IV})$$

where M is molecular weight.

COMSOL Multiphysics Version 5.6 (COMSOL, Sweden) was used for simulating the time-dependent diffusion behavior of VEGF in bioprinted tissue. The geometry of the bioprinted tissue and surrounding culture medium were modeled using the Solidworks 3D CAD software and imported to the COMSOL software. Transport of the dilute-species module was adopted in this study. The diffusion coefficients of the bioprinted tissue and surrounding culture medium were applied as described above.

2.6. Bioprinting of mid-scale vasculature-embedded tissue

Mid-scale vasculature-embedded tissues were printed in a polyethylene terephthalate cell culture insert with a pore size of 8.0 μm (36106; SPL Life Science, South Korea) to generate a biochemical gradient environment in the bioprinted tissue. Additionally, a pressure-sensitive adhesive film (4313663, Thermo Fisher Scientific) was cut into a ring shape with an inner diameter of 5 mm and an outer diameter of 22 mm and attached to the bottom of an insert to create a diffusion channel for the biochemical cocktail through the bioprinted tissue. This makes the biochemicals diffuse only through the diffusion channel. Subsequently, the film-attached inserts were soaked in 70%

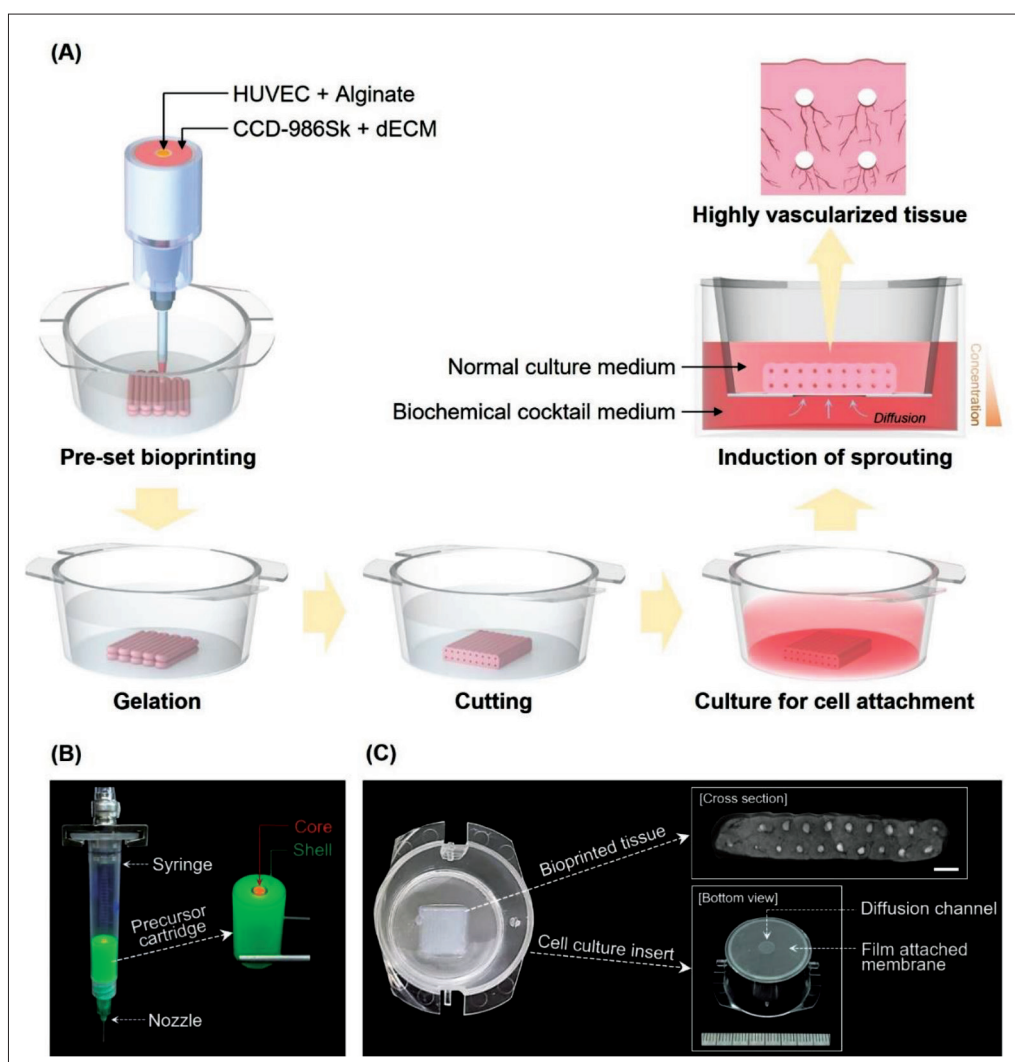


Figure 1. (A) Schematic illustration of multi-scale vascularization strategy used in this study. (B) Experimental setup for pre-set extrusion bioprinting and applied coaxial precursor cartridge (detailed images are shown in Figure S2 of Supplementary File). (C) Bioprinted tissue fabricated by pre-set extrusion bioprinting technique and experimental setup for generating a biochemical gradient environment in bioprinted tissue. Scale bar: 1 mm.

ethanol for 1 h and subsequently exposed to UV light for 2 h for sterilization before bioprinting.

dECM bioink containing CCD-986Sk cells and alginate bioink containing HUVECs were loaded in the shell and core regions of a precursor cartridge which has core diameter of 1.7 mm. Next, a bioink-loaded precursor cartridge was placed into a 3-mL Luer lock syringe and coupled to a 3D bioprinting system (3DX Bioprinter, T&R Biofab). The working pressure and temperature for bioprinting were 7–9 kPa and 4°C, respectively, and the nozzle was 18G. The tissue was printed into an insert containing 25°C DPBS to a size of 10 × 10 × 1.6 mm and a two-layer structure with a diffusion channel in the center. After bioprinting, the tissue was gelated in a CO₂ incubator for 1 h (Figure S1). Finally, both perpendicular sides with

mid-scale vasculatures of the bioprinted tissue were cut using a surgical blade to remove embedded alginate bioink, and DPBS was replaced with EGM-2 culture medium, as described in Figure 1A.

2.7. Induction of endothelial sprouting

The biochemical cocktail was prepared by supplementing EGM-2 with 75 ng/mL VEGF (293-VE, R&D Systems, USA), 150 ng/mL phorbol 12-myristate 13-acetate (P8139, Sigma-Aldrich), and 500 nM sphingosine-1-phosphate (73914, Sigma-Aldrich). The biochemical cocktail was added to the underside of the transwell, and normal EGM-2 medium was added to the insert after 3 days of bioprinting. The bioprinted tissues were cultured in a CO₂ incubator, and the biochemical cocktail and EGM-2 medium were changed every 24 h.

2.8. Fluorescence staining of bioprinted tissue

For assessing cell viability, live and dead staining was performed on the bioprinted tissue. The culture medium was removed from the bioprinted tissue and rinsed three times with prewarmed DPBS. Cells were then stained with calcein-AM (C1430, Thermo Fisher Scientific) and ethidium homodimer-1 (E1169, Thermo Fisher Scientific) solution for 40 min at 25°C.

In addition, the bioprinted tissue was stained with CD31 and alpha-smooth muscle actin for visualizing the vasculatures and the surrounding CCD-986Sk cells. Briefly, the culture medium was removed from the samples and rinsed with DPBS. The sample was then fixed with 4% paraformaldehyde solution for 5 min and washed with DPBS five times. Then, the sample was soaked in a 0.25% Triton X-100 solution for 1 min for permeabilization. For blocking, the permeabilized sample was soaked in a 1% bovine serum albumin solution for 1 h. Subsequently, the samples were immunostained with CD31 (ab9498, Abcam, UK) and α -SMA (ab124964, Abcam) primary antibodies for 12 h. Alexa Fluor 488 anti-mouse goat (ab150113, Abcam) and Alexa Fluor 594 anti-rabbit goat (ab150080, Abcam) secondary antibodies were stained for 2 h. Finally, the nuclei of cells in the bioprinted construct were stained with Hoechst 33342 (62249, Thermo Fisher Scientific). All fluorescently stained tissues were subjected to laser scanning confocal microscopy (FV1200; Olympus).

3. Results and discussion

Figure 1A shows the vascularization strategy used in this study for fabricating bioprinted tissue. The mid-scale vasculatures were created in bioprinted tissue using a pre-set extrusion bioprinting technique (Figure 1B). Subsequently, the bioprinted tissue was cultured for the attachment of cells. Next, we designed an experimental setup for generating a biochemical gradient in bioprinted tissue (Figure 1C). As a result, the endothelial cells formed perfusable capillary branches.

Pre-set extrusion bioprinting is a derivative technique from extrusion-based bioprinting method^[12]. The resolution of conventional extrusion bioprinting is lower than other bioprinting method such as jetting-based^[13] and polymerization-based^[14] bioprinting method. For this reason, conventional extrusion bioprinting is not effective for building mid-scale lumen demonstrated in this paper. On the other hand, pre-set extrusion bioprinting has high resolution that is able to build lumen with a diameter of 185–445 μm in bioprinted tissue (Figure 2A and B) by simply using a coaxial core-shell precursor cartridge, which is a major advantage of pre-set extrusion bioprinting. Also, coaxial nozzle-assisted bioprinting, a common extrusion-

based bioprinting method for fabricating vascularized tissue constructs^[15] requires two bioink supply equipment, *i.e.*, pneumatic dispenser and syringe pump. On the other hand, only a pneumatic dispenser is required for pre-set extrusion bioprinting with coaxial core-shell precursor cartridge to fabricate mid-scale vasculature-embedded tissue. Therefore, fabricating mid-scale vasculature-embedded tissue using pre-set extrusion bioprinting is more cost-effective than coaxial nozzle-assisted bioprinting technique.

Furthermore, pre-set extrusion bioprinting can be used for controlling the diameter of the vasculature by adjusting the concentration of the bioink and the geometry of the precursor cartridge. In this technique, the similarity in the shear viscosity of bioinks in a precursor cartridge is important because it determines the co-printability of the bioinks^[9]. Within the co-printable range (Figure S3), the areal proportion of cross section of the printed construct, fabricated by the pre-set extrusion bioprinting technique, is controlled by adjusting the concentration of each bioink because of the difference in shear viscosity. Considering this possibility, the lumen size in the printed construct was controllable (Figure 2A). When the concentration of the sacrificial bioink (alginate) was diluted, a larger lumen was generated, because the viscosity of the alginate solution decreased with dilution (Figure S4). Another method for changing the lumen size in a printed construct is changing the geometry of the precursor cartridge (Figure 2B). The results showed that a small change in the area of the core region of a precursor cartridge caused large differences in the area of the lumen in the bioprinted construct. This result can be attributed to the geometry of the core-shell precursor cartridge and syringe.

The printed tissue construct had high initial cell viability (Figure 2C). Coaxial nozzle-assisted bioprinting sometimes requires a small-diameter nozzle in the core region for fabrication of small vasculature-embedded tissue. When cells in the bioink are extruded through a small-diameter nozzle, they can be damaged by shear stress^[16]. However, in the pre-set extrusion bioprinting process, small-vasculature-embedded tissue can be fabricated by adjusting the concentration of bioink and the geometry of the precursor cartridge without a small-diameter nozzle. Thus, the pre-set extrusion bioprinting technique has a high potential for fabricating tissue constructs with embedded small-diameter vasculatures with high cell viability. In addition, endothelial cells were well attached to the inner surface of the lumen (Figure 2D) and proliferated to form mid-scale vasculature in the culture (Figure 2E). Although the pre-set extrusion bioprinting technique is capable of fabricating mid-scale vasculature-embedded tissue, it is not effective for capillary branches in the native tissue.

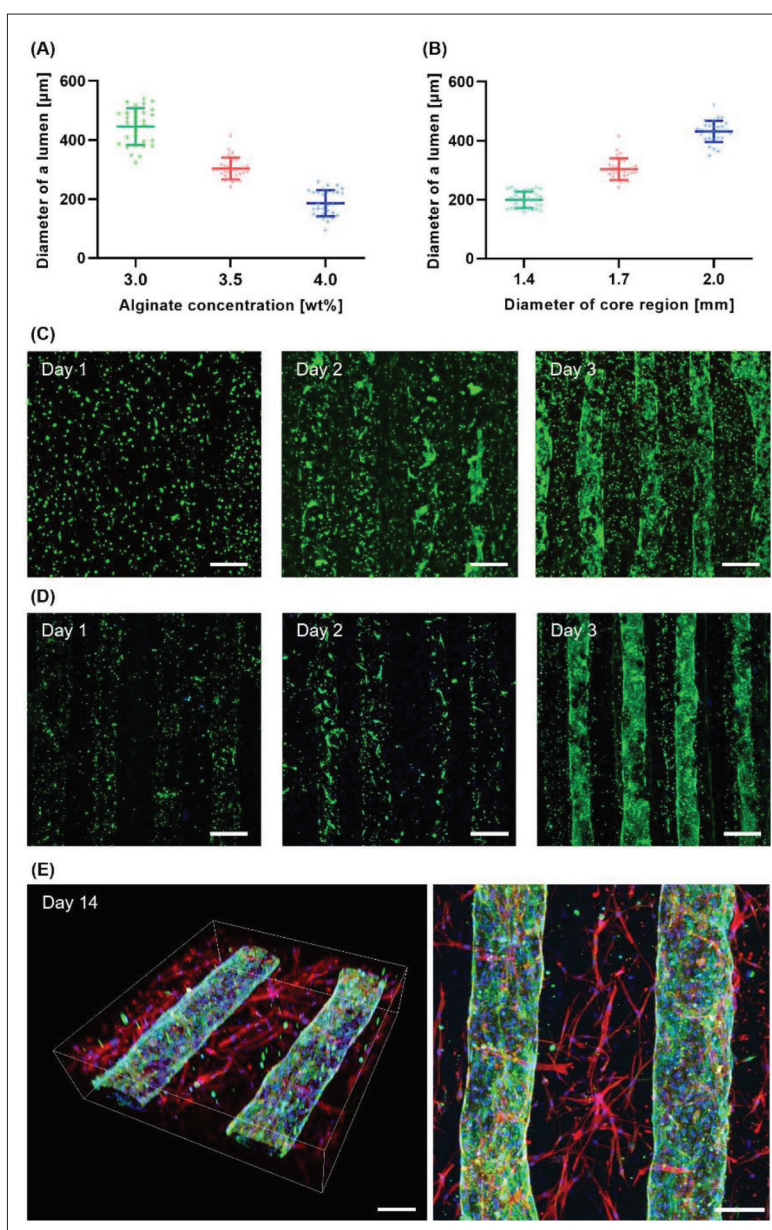


Figure 2. Demonstration of pre-set extrusion bioprinting technique as the fabrication method for mid-scale vasculature-embedded tissue. (A) Changes of lumen diameter in bioprinted tissue with alginate concentration (diameter of core region: 3.5 mm, $n = 30$). (B) Influence of geometry of coaxial precursor cartridge on fabricated lumen diameter in bioprinted tissue (concentration of alginate solution: 3.5%, $n = 30$). (C) Live/dead staining result for bioprinted tissue. Green: calcein-AM; red: ethidium homodimer-1; scale bar: 300 μm. (D) Immunostaining result for bioprinted tissue. Green: CD31; Blue: nucleus; scale bar: 300 μm. (E) Formation of endothelialized mid-scale vasculatures in bioprinted tissue via pre-set extrusion bioprinting technique. Red: alpha-smooth muscle actin; green: CD31; blue: nucleus; scale bar: 200 μm.

Therefore, we aimed to generate a biochemical gradient in the bioprinted tissue to induce endothelial cell sprouting and capillary formation.

To generate a biochemical gradient in the bioprinted tissue, we modified the cell culture insert to create a diffusion channel and bioprinted tissue in the cell culture insert. A computational fluid dynamics simulation of diffusion was

applied to confirm the biochemical gradient environment in the bioprinted tissue. Before the simulation, the effective diffusion coefficient of VEGF through the dECM bioink was derived experimentally (Figure 3A). The effective diffusion coefficient of VEGF through the dECM bioink was $1.25 \times 10^{-11} \text{ m}^2/\text{s}$, as derived from the data shown in Figure 3B, which is within a reasonable range on the basis of previous studies^[17,18]. The effective diffusion coefficient

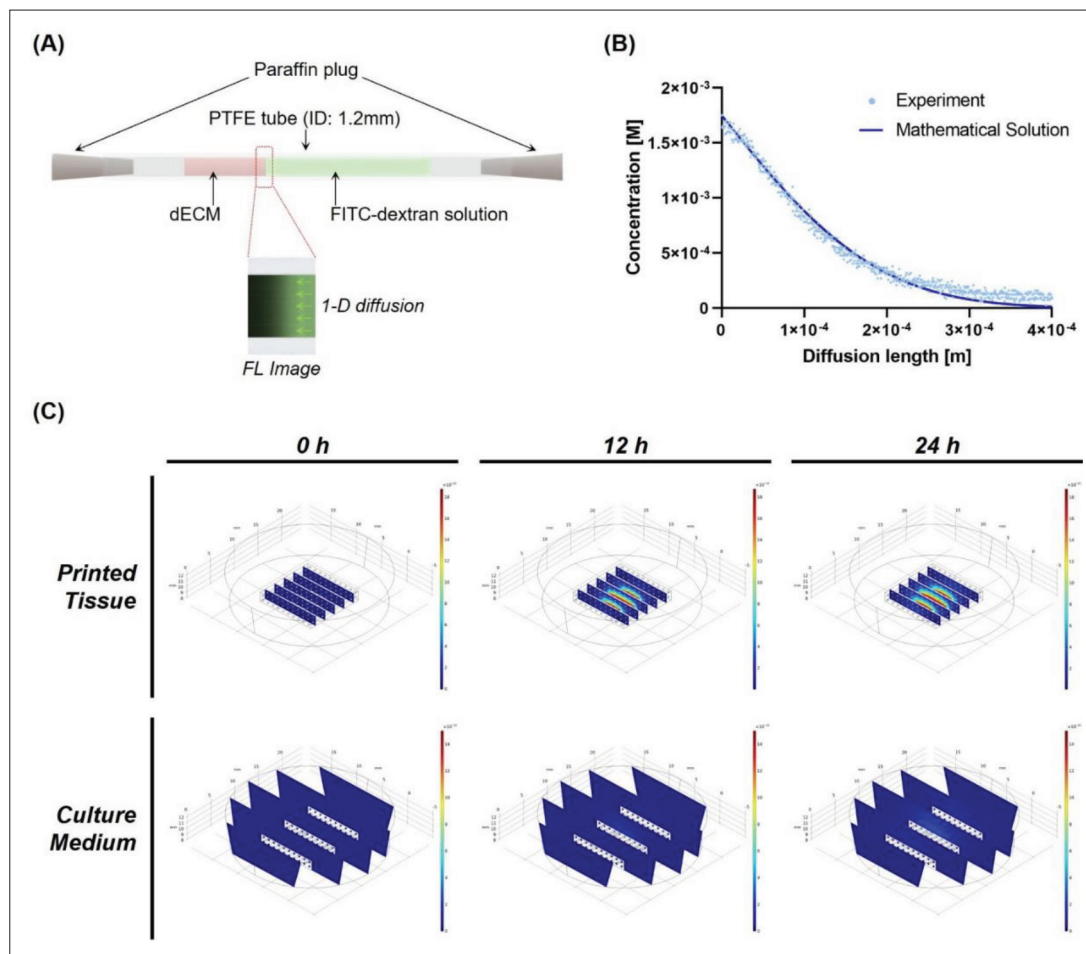


Figure 3. (A) Experimental setup for deriving the effective diffusion coefficient of FITC-dextran through dECM bioink. (B) One-dimensional FITC-dextran concentration profile from experimental data and theoretical profile. (C) Time-dependent simulation results for diffusion of VEGF through bioprinted tissue and culture medium (details are described in [Figures S6 and S7](#) of Supplementary File).

of VEGF in the culture medium was $1.46 \times 10^{-10} \text{ m}^2/\text{s}$. These effective diffusion coefficients of VEGF were used for simulating the diffusion behavior of VEGF in the bioprinted tissue ([Figure 3C](#)). The biochemical gradient environment was generated in the bioprinted tissue and maintained for 24 h as intended ([Figure S5](#)). Furthermore, because the biochemical cocktail and normal EGM-2 medium were changed every 24 h, the biochemical gradient environment in bioprinted tissue could be maintained for entire experimental periods.

We set up two different groups: the first was the experimental group in which sprouting was induced, and the second was the control group, which was cultured with normal EGM-2 medium ([Figure 4](#)). Endothelial cells on the surface of the lumen proliferated up to days 10 in both groups ([Figure 5A](#)). Subsequently, endothelial cells sprouted from the lumen in the experimental group because of the biochemical gradient environment; however,

endothelial cells in the control group did not sprout. Sprouted endothelial cells were located in the interstitial tissue, forming a highly vascularized tissue at days 14 ([Figure 5B](#); [Videoclip S1](#)). Since the concentration of biochemicals at the center and the peripheral of bioprinted tissue was different ([Figure S5](#)), a different vascularization rate was observed on each part.

VEGF is a growth factor related to angiogenesis and vasculogenesis. In addition, phorbol 12-myristate 13-acetate promotes the secretion of collagenase from endothelial cells, and sphingosine-1-phosphate stimulates the proliferation and migration of endothelial cells^[7]. Owing to the roles of these biochemicals and their gradient environment, endothelial cells not only sprouted from the mid-scale vasculatures in the bioprinted tissue, but also formed perfusable capillary branches with a diameter of $19.57 \mu\text{m}$ ([Figure S6](#)). Fluorescence micro-particles (R0100, Thermo Fisher Scientific), injected into the

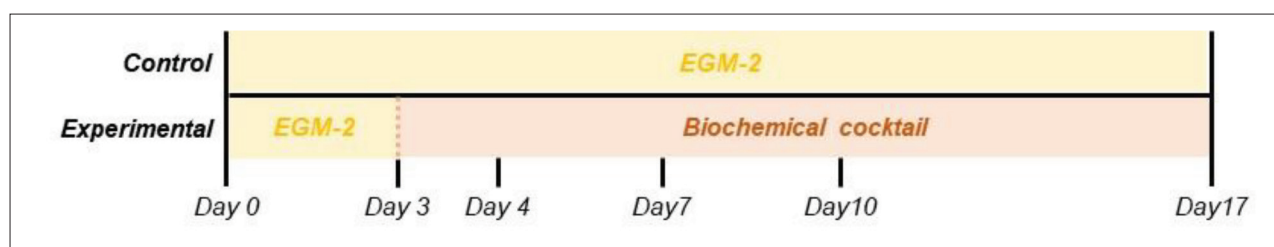


Figure 4. The culture media used during the experiment and at the sample observation timepoints for each group. Inducement of endothelial sprouting was conducted for 14 days (from days 3 to 17).

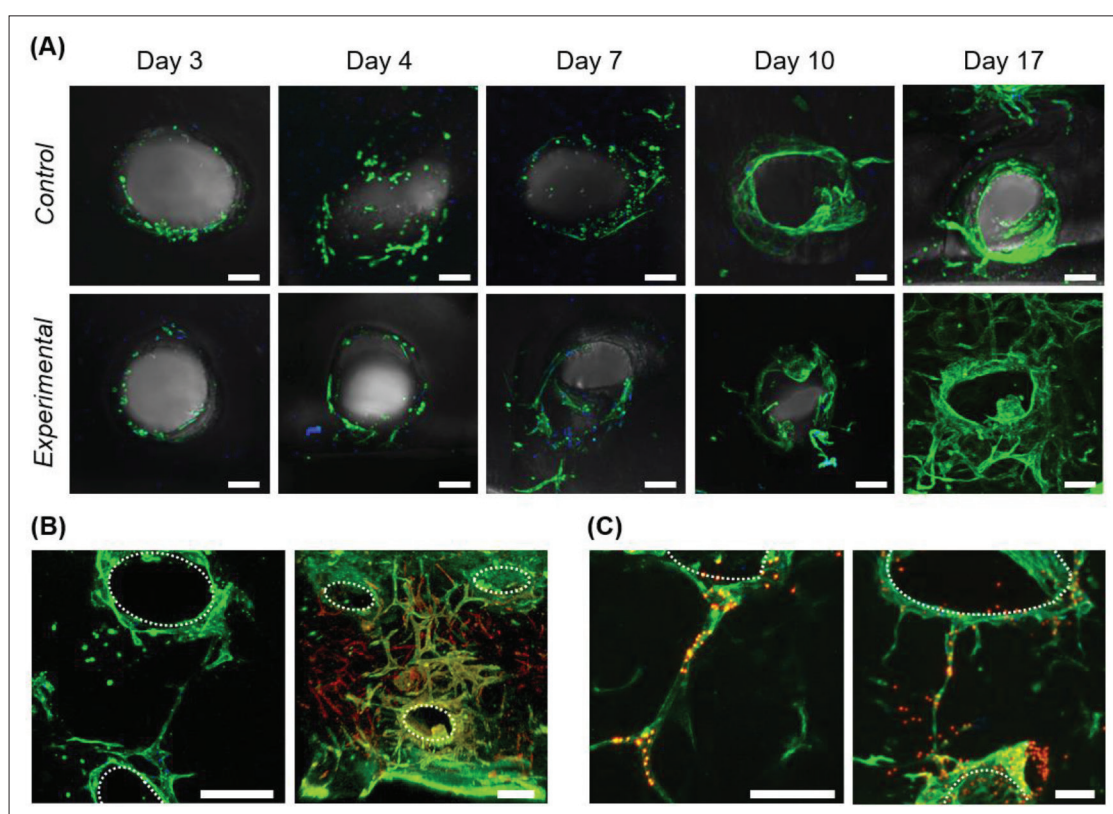


Figure 5. Induction of endothelial sprouting on bioprinted tissue. (A) Observation of a lumen during the experiment. Green: CD31; blue: nucleus; scale bar: 100 μ m. (B) Endothelial sprouting after 14 days of induction of endothelial sprouting. Left image shows the peripheral view while right image shows the center of bioprinted tissue. Green: CD31; red: alpha-smooth muscle actin; white dash line: lumen; scale bar: 200 μ m. (C) Material transfer in bioprinted tissue. Green: CD31; red: fluorescence particle; white dash line: lumen; scale bar: 100 μ m.

vascularized tissue, were transported through mid-scale vasculatures and capillaries (Figure 5C). Furthermore, some mid-scale vasculatures were interconnected with the sprouted capillary branches (Videoclip S2).

Although we demonstrated a strategy to build multi-scale vascularized tissue, our study has certain limitations that need to be addressed. Since we focused on demonstrating multi-scale vascularization strategy developed in this study, the major factors which influence the degree of vascularization, such as stiffness of matrix, concentration

of growth factor, and bioprinted lumen size and its pattern, were not evaluated. To fabricate vascularized tissue more effectively with the strategy developed in this research, these major factors should be investigated through further research. We did not evaluate vascularized tissue function. Although the tissue fabricated in this study has numerous vasculatures, biochemicals can influence the cells in the interstitial tissue^[19]; therefore, the functionality of cells in interstitial tissue needs to be evaluated. Another challenge for further research is the induction of connections between vasculatures to build the vascular network. The capillaries

in the tissue fabricated in this study were formed radially from the diffusion channel created by modifying the cell culture insert; therefore, interconnecting each vasculature is difficult. A recent report showed that the direction of a sprouted capillary can be controlled by engineering the stiffness of the bioink^[20]. Upon combining this approach with the strategy suggested in this research, a multi-scale vascular network-like native tissue can be built in the bioprinted tissue. Another challenge is the formation of large-scale blood vessels in the tissue for anastomosis. In organ transplantation, a large-scale blood vessel is sometimes necessary to connect with other blood vessels in the body. Szklanny *et al.*^[21] reported a tissue fabrication method using large-scale blood vessels for tissue flaps. This method can be applied together with our vascularization strategy for fabricating a tissue with a hierarchical blood vessel structure and a large-mid-small-sized structure.

5. Conclusion

This study successfully demonstrated an advanced multi-scale vascularization strategy through a combination of pre-set extrusion bioprinting and endothelial sprouting by biochemical factors. Using this strategy, we successfully fabricated bioprinted tissue embedded with hierarchical vascular structures consisting of mid-scale vasculatures and capillary branches. In particular, vasculatures, with a diameter of hundreds of micrometers, formed by the pre-set extrusion bioprinting technique, and capillary branches, with a diameter of tens of micrometers, formed by endothelial sprouting, were able to effectively deliver materials, such as oxygen and nutrients to cells. In conclusion, the strategy for multi-scale vascularization in bioprinted tissue demonstrated in this work is expected to become a useful technology for bioartificial tissue or organ development.

Acknowledgments

None.

Funding

This research was supported by a National Research Foundation of Korea (NRF) grant funded by the Ministry of Education (NRF-2017R1A6A1A03015562) and Ministry of Science and ICT (NRF-2020R1A2B5B01002716).

Conflict of interest

The authors declare no conflicts of interest.

Author contributions

Conceptualization: Songwan Jin

Formal analysis: Songwan Jin, Jae-Hun Kim

Funding acquisition: Won-Soo Yun

Investigation: Jae-Hun Kim, Minji Park

Methodology: Songwan Jin, Jae-Hun Kim

Project administration: Songwan Jin

Writing – original draft: Jae-Hun Kim, Minji Park

Writing – review & editing: Songwan Jin, Won-Soo Yun, Jin-Hyung Shim

Ethics approval and consent to participate

Not applicable.

Consent for publication

Not applicable.

Availability of data

Data can be obtained from the corresponding author upon reasonable request.

References

1. Ng WL, Chua CK, Shen Y-F, 2019, Print me an organ! Why we are not there yet. *Prog Polym Sci*, 97:101145.
<https://doi.org/10.1016/j.progpolymsci.2019.101145>
2. Griffith BP, Goerlich CE, Singh AK, et al., 2022, Genetically modified porcine-to-human cardiac xenotransplantation. *N Engl J Med*, 387(1):35–44.
<https://doi.org/10.1056/NEJMoa2201422>
3. Cohen BP, Bernstein JL, Morrison KA, et al., 2018, Tissue engineering the human auricle by auricular chondrocyte-mesenchymal stem cell co-implantation. *PLoS One*, 13(10):e0202356.
<https://doi.org/10.1371/journal.pone.0202356>
4. Uygun BE, Soto-Gutierrez A, Yagi H, et al., 2010, Organ reengineering through development of a transplantable recellularized liver graft using decellularized liver matrix. *Nat Med*, 16(7):814–820.
<https://doi.org/10.1038/nm.2170>
5. Di Piazza E, Pandolfi E, Cacciotti I, et al., 2021, Bioprinting technology in skin, heart, pancreas and cartilage tissues: Progress and challenges in clinical practice. *Int J Environ Res Public Health*, 18(20):10806.
<https://doi.org/10.3390/ijerph182010806>
6. Miri AK, Khalilpour A, Cecen B, et al., 2019, Multiscale bioprinting of vascularized models. *Biomaterials*, 198: 204–216.
<https://doi.org/10.1016/j.biomaterials.2018.08.006>
7. van Duinen V, Stam W, Mulder E, et al., 2020, Robust and scalable angiogenesis assay of perfused 3D human iPSC-

- derived endothelium for anti-angiogenic drug screening. *Int J Mol Sci*, 21(13):4804.
<https://doi.org/10.3390/ijms21134804>
8. Kang D, Ahn G, Kim D, et al., 2018, Pre-set extrusion bioprinting for multiscale heterogeneous tissue structure fabrication. *Biofabrication*, 10(3):035008.
<https://doi.org/10.1088/1758-5090/aac70b>
 9. Kang D, Hong G, An S, et al., 2020, Bioprinting of multiscaled hepatic lobules within a highly vascularized construct. *Small*, 16(13):e1905505.
<https://doi.org/10.1002/sml.201905505>
 10. Hettiaratchi MH, Schudel A, Rouse T, et al., 2018, A rapid method for determining protein diffusion through hydrogels for regenerative medicine applications. *APL Bioeng*, 2(2):026110.
<https://doi.org/10.1063/1.4999925>
 11. Erickson HP, 2009, Size and shape of protein molecules at the nanometer level determined by sedimentation, gel filtration, and electron microscopy. *Biol Proced Online*, 11:32–51.
<https://doi.org/10.1007/s12575-009-9008-x>
 12. Ozbolat IT, Hospodiuk M., 2016 Current advances and future perspectives in extrusion-based bioprinting. *Biomaterials*, 76:321–343.
<https://doi.org/10.1016/j.biomaterials.2015.10.076>
 13. Ng WL, Huang X, Shkolnikov V, et al., 2021, Controlling droplet impact velocity and droplet volume: Key factors to achieving high cell viability in sub-nanoliter droplet-based bioprinting. *Int J Bioprint*, 8(1):424.
<http://dx.doi.org/10.18063/ijb.v8i1.424>
 14. Ng WL, Lee JM, Zhou M, et al., 2020, Vat polymerization-based bioprinting—Process, materials, applications and regulatory challenges. *Biofabrication*, 12(2):022001.
<https://doi.org/10.1088/1758-5090/ab6034>
 15. Gao Q, He Y, Fu J, et al., 2015, Coaxial nozzle-assisted 3D bioprinting with built-in microchannels for nutrients delivery. *Biomaterials*, 61:203–215.
<https://doi.org/10.1016/j.biomaterials.2015.05.031>
 16. Han S, Kim CM, Jin S, et al., 2021, Study of the process-induced cell damage in forced extrusion bioprinting. *Biofabrication*, 13(3).
<https://doi.org/10.1088/1758-5090/ac0415>
 17. Rosenblatt J, Rhee W, Wallace D, 1989, The effect of collagen fiber size distribution on the release rate of proteins from collagen matrices by diffusion. *J Control Release*, 9(3): 195–203.
[https://doi.org/10.1016/0168-3659\(89\)90088-6](https://doi.org/10.1016/0168-3659(89)90088-6)
 18. Ramanujan S, Pluen A, McKee TD, et al., 2002, Diffusion and convection in collagen gels: Implications for transport in the tumor interstitium. *Biophys J*, 83(3):1650–1660.
[https://doi.org/10.1016/S0006-3495\(02\)73933-7](https://doi.org/10.1016/S0006-3495(02)73933-7)
 19. Seo Y, Baba H, Fukuda T, et al., 2000, High expression of vascular endothelial growth factor is associated with liver metastasis and a poor prognosis for patients with ductal pancreatic adenocarcinoma. *Cancer*, 88(10):2239–2245.
[https://doi.org/10.1002/\(sici\)1097-0142\(20000515\)88:10<2239::aid-cncr6>3.0.co;2-v](https://doi.org/10.1002/(sici)1097-0142(20000515)88:10<2239::aid-cncr6>3.0.co;2-v)
 20. Son J, Hong SJ, Lim JW, et al., 2021, Engineering tissue-specific, multiscale microvasculature with a capillary network for prevascularized tissue. *Small Methods*, 5(10):e2100632.
<https://doi.org/10.1002/smt.202100632>
 21. Szklanny AA, Machour M, Redenski I, et al., 2021, 3D bioprinting of engineered tissue flaps with hierarchical vessel networks (VesselNet) for direct host-to-implant perfusion. *Adv Mater*, 33(42):e2102661.
<https://doi.org/10.1002/adma.202102661>